J|A|C|S
ARTICLES
Published on Web 05/02/2007

Evidence from Raman Spectroscopy That InhA, the Mycobacterial Enoyl Reductase, Modulates the Conformation of the NADH Cofactor to Promote Catalysis

Alasdair F. Bell,[†] Christopher F. Stratton,[‡] Xujie Zhang, Polina Novichenok, Andrew A. Jaye, Pravin A. Nair,[§] Sapan Parikh, Richa Rawat, and Peter J. Tonge*

Contribution from the Department of Chemistry, Stony Brook University, Stony Brook, New York 11794-3400

Received November 22, 2006; E-mail: peter.tonge@sunysb.edu

Abstract: InhA, the enoyl reductase from *Mycobacterium tuberculosis*, catalyzes the NADH-dependent reduction of *trans*-2-enoyl-ACPs. In the present work, Raman spectroscopy has been used to identify catalytically relevant changes in the conformation of the nicotinamide ring that occur when NADH binds to InhA. For 4(*S*)-NADD, there is an 11 cm^{-1} decrease in the wavenumber of the C4−D stretching band (ν_{C-D}) and a 50% decrease in the width of this band upon binding to InhA. While a similar reduction in line width is observed for the corresponding band arising from 4(*R*)-NADD, ν_{C-D} for this isomer increases 34 cm^{-1} upon binding to InhA. These changes in ν_{C-D} indicate that the nicotinamide ring adopts a bound conformation in which the 4(*S*)C−D bond is in a pseudoaxial orientation. Mutagenesis of F149, a conserved active site residue close to the cofactor, demonstrates that this enzyme-induced modulation in cofactor structure is directly linked to catalysis. In contrast to the wild-type enzyme, Raman spectra of NADD bound to F149A InhA resemble those of NADD in solution. Consequently, F149A is no longer able to optimally position the cofactor for hydride transfer, which correlates with the 30-fold decrease in k_{cat} and 2-fold increase in $^{D}(V/K_{NADH})$ caused by this mutation. These studies thus substantiate the proposal that hydride transfer is promoted by pseudoaxial positioning of the NADH pro-4S bond, and indicate that catalysis of substrate reduction by InhA results, in part, from correct orientation of the cofactor in the ground state.

Introduction

InhA, the enoyl reductase from *Mycobacterium tuberculosis* and a member of the short-chain dehydrogenase/reductase (SDR) family,[1−3] catalyzes the NADH-dependent reduction of long-chain *trans*-2-enoyl-ACP fatty acids in the type II fatty acid biosynthesis pathway of *M. tuberculosis* (Scheme 1). This enzyme is a target for isoniazid, a front-line antituberculosis drug which inhibits the biosynthesis of mycolic acids, thereby compromising cell wall integrity.[4−7] Experiments utilizing a temperature-sensitive mutant of InhA have validated this enzyme as an excellent target for anti-TB drug discovery, and consequently a detailed understanding of the catalytic mechanism is important for directing the design of potent InhA inhibitors.[8,9]

Scheme 1

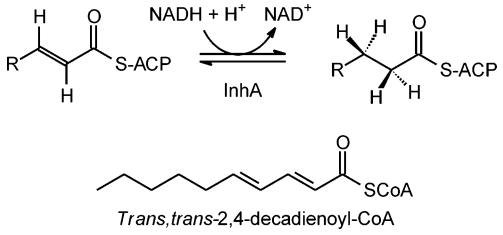

All members of the SDR family contain a conserved catalytic triad which includes a tyrosine and a lysine residue. In InhA, these residues are Y158 and K165 (Figure 1).[2] Similar to the dehydrogenases, structural and kinetic studies have revealed that K165 in InhA functions primarily in cofactor binding, forming hydrogen bonds with the nicotinamide ribose 2′ and 3′ hydroxyl groups.[5,10] In addition, crystallographic data suggests that Y158 facilitates catalysis by stabilizing the enolate intermediate which

[†] Present address: Medarex Inc., Sunnyvale, CA 94041.
[‡] Present address: Department of Chemistry and Chemical Biology, Cornell University, Ithaca, NY 14853.
[§] Present address: Memorial Sloan Kettering Cancer Center, New York, NY 10021.

(1) Nakajin, S.; Takase, N.; Ohno, S.; Toyoshima, S.; Baker, M. E. *Biochem. J.* **1998**, *334*, 553−557.
(2) Rozwarski, D. A.; Vilcheze, C.; Sugantino, M.; Bittman, R.; Sacchettini, J. C. *J. Biol. Chem.* **1999**, *274*, 15582−15589.
(3) Oppermann, U.; Filling, C.; Hult, M.; Shafqat, N.; Wu, X.; Lindh, M.; Shafqat, J.; Nordling, E.; Kallberg, Y.; Persson, B.; Jornvall, H. *Chem. Biol. Interact.* **2003**, *143−144*, 247−253.
(4) Banerjee, A.; Dubnau, E.; Quemard, A.; Balasubramanian, V.; Um, K. S.; Wilson, T.; Collins, D.; de Lisle, G.; Jacobs, W. R., Jr. *Science* **1994**, *263*, 227−230.
(5) Dessen, A.; Quemard, A.; Blanchard, J. S.; Jacobs, W. R., Jr.; Sacchettini, J. C. *Science* **1995**, *267*, 1638−1641.
(6) Quemard, A.; Sacchettini, J. C.; Dessen, A.; Vilcheze, C.; Bittman, R.; Jacobs, W. R., Jr.; Blanchard, J. S. *Biochemistry* **1995**, *34*, 8235−8241.
(7) Basso, L. A.; Zheng, R.; Musser, J. M.; Jacobs, W. R., Jr.; Blanchard, J. S. *J. Infect. Dis.* **1998**, *178*, 769−775.
(8) Vilcheze, C.; Morbidoni, H. R.; Weisbrod, T. R.; Iwamoto, H.; Kuo, M.; Sacchettini, J. C.; Jacobs, W. R., Jr. *J. Bacteriol.* **2000**, *182*, 4059−4067.
(9) Sullivan, T. J.; Truglio, J. J.; Boyne, M. E.; Novichenok, P.; Zhang, X.; Stratton, C. F.; Li, H.-J.; Kaur, T.; Amin, A.; Johnson, F.; Slayden, R. A.; Kisker, C.; Tonge, P. J. *ACS Chem. Biol.* **2006**, *1*, 43−53.
(10) Parikh, S.; Moynihan, D. P.; Xiao, G.; Tonge, P. J. *Biochemistry* **1999**, *38*, 13623−13634.

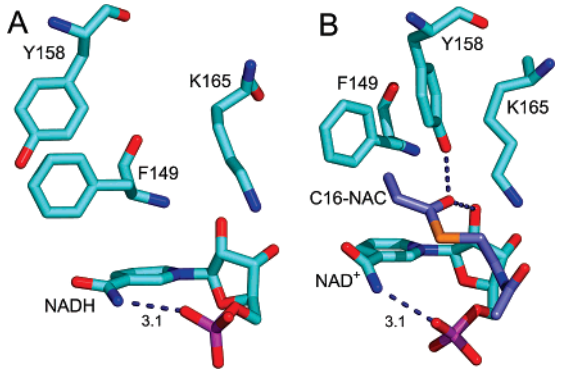

Figure 1. (A) Position of F149, Y158, and K165 in a binary complex of InhA with NADH taken from Dessen et al. (ref 5) (PDB code: 1ENY). (B) Ternary complex with a C16 substrate and NAD^+. Although the only available ternary complexes of InhA involve NAD^+ and not NADH, a ternary complex structure is presented in order to show the rotation of Y158 that occurs upon substrate binding (PDB code: 1BVR) (ref 2). In both structures the NAD(H) is bound in the anti conformation such that the amide group forms a hydrogen bond with an NAD(H) phosphate oxygen. The figure was made with pymol (ref 36).

forms during hydride transfer.[2] However, while replacement of Y158 with Phe reduces k_{cat} 24-fold, the Y158S mutant has wild-type activity, bringing into question the ultimate importance of this residue in catalysis.[10,11]

In the dehydrogenases the third residue in the catalytic triad is a Ser or Thr, while in the enoyl reductases this residue is either a Phe or a Tyr (F149 in InhA). In UDP-galactose-4-epimerase the conserved Ser (S124) functions together with Y149 to reversibly protonate and deprotonate the ketone oxygen of the substrate.[12,13] However, the role of the conserved Phe/Tyr in the reductases is less clear. In the crystal structure of the NADH−InhA complex, the cofactor is observed to bind at the bottom of a large open cavity with the side chain of F149 lying just above the nicotinamide ring.[5] Based on structural data, Rozwarski et al. have proposed that F149 protects the substrate from adventitious attack by water.[2]

In order to further investigate the role of F149 in catalysis, we have used Raman spectroscopy to probe the structure and dynamics of 4(*R*)- and 4(*S*)-NADD and a substrate analog, *trans*,*trans*-2,4-decadienoyl-CoA (Scheme 1), bound to the wild-type enzyme and the F149A mutant. An advantage of this approach is that the Raman effect is instantaneous, and thus Raman spectra are not susceptible to conformational averaging but contain a snapshot of all species present at any instant. Callender and co-workers have demonstrated that the C4−D stretching vibration (ν_{C-D}) of stereospecifically deuterium-labeled NADD is an excellent probe of the influence of the environment on the cofactor, as this is an isolated vibration with little or no vibrational coupling to other normal coordinates.[14−17] In addition, our numerous studies on two β-oxidation enzymes, enoyl-CoA hydratase (ECH) and medium-chain acyl-CoA dehydrogenase (MCAD), provide a detailed framework for interpreting data on the binding of the diene substrate analog to InhA.[18−21]

In the present work we demonstrate that InhA binds NADD in a conformation that is optimized for hydride transfer. In addition, the Raman studies, coupled with kinetic isotope effect data, demonstrate that F149 plays a key role in modulating both the structure and reactivity of NADH(D) when bound to InhA.

Materials and Methods

Materials. Coenzyme A (CoA) lithium salt, β-NADH, β-NAD^+, equine liver alcohol dehydrogenase (EC 1.1.1.1), and glucose-6-phosphate dehydrogenase type XXIV from *L. mesenteroides* were purchased from Sigma Chemical company. [1-D]-Glucose (98% D) was from Cambridge Isotopes Labs (Andover, MA). *trans*,*trans*-2,4-Decadienal was purchased from Aldrich Chemical Co. Sephadex G-25 (fine) was purchased from Pharmacia Biotech (Uppsala, Sweden). His-Bind resin was from Novagen (Madison, WI). Oligonucleotides were purchased from IDT, Inc. (Coralville, IA). Spin columns were purchased from Princeton Separations Inc. (Adelphia, NJ). DNA purification kits were from Qiagen Inc. (Valencia, OH). Ethanol-d_6 (99% D), all other buffers and salts (reagent grade and better), solvents (HPLC grade or better), and chemicals were purchased from Fisher Scientific Co. (Pittsburgh, PA).

Synthesis of Substrates and Substrate Analogs. *trans*,*trans*-2,4-Decadienoic acid was synthesized from the aldehyde by oxidation with $AgNO_3$ in the presence of 10% NaOH.[22,23] Briefly, 0.93 g of silver nitrate in 3.5 mL of water was added to a solution of 0.38 g (0.0025 mol) of *trans*,*trans*-2,4-decadienal in 100 mL of ethanol at room temperature followed by the dropwise addition of 22 mL of 0.5 M NaOH. After stirring overnight at room temperature, the insoluble material was removed by filtration, and the solution was concentrated in vacuo. The alkaline solution was extracted with diethyl ether and then acidified with dilute HCl to precipitate the product which was obtained by filtration. ^{1}H NMR (500 MHz, CDCl3): δ 11.76 (s, 1H), 7.35 (m, 1H), 6.19 (m, 2H), 5.79 (d, 1H Jtrans = 16.0 Hz 3J = 3.0 Hz), 2.19 (q, 2H 3J = 6.6 Hz), 1.43 (m, 2H), 1.29 (m, 4H), 0.88 (t, 3H 3J = 6.6 Hz).

trans,*trans*-2,4-Decadienoyl-CoA (decadienoyl-CoA) was synthesized from the respective acid using the method described previously for hexadienoyl-CoA[19,24] and had an A_{265}/A_{296} ratio of 1.13. *trans*-2-Dodecenoyl-CoA (DD-CoA) was synthesized from the respective acid using the mixed anhydride method,[6,10] and DD-CoA was then used for the synthesis of *trans*-2-dodecenoyl-acyl carrier protein (DD-ACP) as described.[25]

Synthesis of 4(*S*)- and 4(*R*)-NADD. 4(*S*)-NADD was synthesized enzymatically by the reduction of NAD^+ with *L. mesenteroides* glucose-6-phosphate dehydrogenase as described previously.[26,27] 4(*R*)-NADD was synthesized from NAD^+ and ethanol-d_6 in the presence of equine liver alcohol dehydrogenase as described previously (31). Both reduced nucleotides were purified as described previously[10] except that the

(11) Fillgrove, K. L.; Anderson, V. E. *Biochemistry* **2001**, *40*, 12412−12421.
(12) Liu, Y. J.; Thoden, J. B.; Kim, J.; Berger, E.; Gulick, A. M.; Ruzicka, F. J.; Holden, H. M.; Frey, P. A. *Biochemistry* **1997**, *36*, 10675−10684.
(13) Thoden, J. B.; Gulick, A. M.; Holden, H. M. *Biochemistry* **1997**, *36*, 10685−10695.
(14) Deng, H.; Zheng, J.; Sloan, D.; Burgner, J.; Callender, R. *Biochemistry* **1992**, *31*, 5085−5092.
(15) Deng, H.; Burgner, J.; Callender, R. *J. Am. Chem. Soc*. **1992**, *114*, 7997−8003.
(16) Chen, Y. Q.; van Beek, J.; Deng, H.; Burgner, J.; Callender, R. *J. Phys. Chem. B* **2002**, *106*, 10733−10740.
(17) van Beek, J.; Deng, H.; Callender, R.; Burgner, J. J. *Raman Spectrosc.* **2002**, *33*, 397−403.
(18) Pellett, J. D.; Sabaj, K. M.; Stephens, A. W.; Bell, A. F.; Wu, J.; Tonge, P. J.; Stankovich, M. T. *Biochemistry* **2000**, *39*, 13982−13992.
(19) Bell, A. F.; Wu, J.; Feng, Y.; Tonge, P. J. *Biochemistry* **2001**, *40*, 1725−1733.
(20) Bell, A. F.; Feng, Y.; Hofstein, H. A.; Parikh, S.; Wu, J.; Rudolph, M. J.; Kisker, C.; Whitty, A.; Tonge, P. *J. Chem. Biol.* **2002**, *9*, 1247−1255.
(21) Wu, J.; Bell, A. F.; Luo, L.; Stephens, A. W.; Stankovich, M. T.; Tonge, P. J. *Biochemistry* **2003**, *42*, 11846−11856.
(22) Sheehan, J. C.; Robinson, C. A. *J. Am. Chem. Soc.* **1951**, *73*, 1207−1210.
(23) Mandai, T.; Gotoh, J.; Otera, J.; Kawada, M. *Chem. Lett.* **1980**, 313−314.
(24) Tonge, P. J.; Anderson, V. E.; Fausto, R.; Kim, M.; PusztaiCarey, M.; Carey, P. R. *Biospectroscopy* **1995**, *1*, 387−394.
(25) Rafi, S.; Novichenok, P.; Kolappan, S.; Zhang, X.; Stratton, C. F.; Rawat, R.; Kisker, C.; Simmerling, C.; Tonge, P. J. *J. Biol. Chem.* **2006**, *281*, 39285−39293.
(26) Viola, R. E.; Cook, P. F.; Cleland, W. W. *Anal. Biochem.* **1979**, *96*, 334−340.
(27) Orr, G. A.; Blanchard, J. S. *Anal. Biochem*. **1984**, *142*, 232−234.

stability of the NADD during purification was improved by performing the anion-exchange chromatography (FPLC, MONO Q HR10/10) at pH 9.0 using 10 mM triethanolamine, rather than pH 7.8.

Enzyme Preparation and Characterization. The F149A mutation was introduced using the QuikChange mutagenesis kit (Stratagene). After verification of the sequence by ABI DNA sequencing, the plasmid was transformed into BL21(DE3)pLysS cells (Novagen) for protein expression. Both wild-type InhA and the F149A mutant were expressed and purified as described previously.[10] Protein concentration was calculated using an ϵ_{280} of 37.3 mM^{-1} cm^{-1} for the wild-type and an ϵ_{280} of 35.9 mM^{-1} cm^{-1} for the F149A mutant.

Steady-State Kinetics for Wild-Type and F149A InhA Proteins. All experiments were performed at 25 °C in 30 mM PIPES and 150 mM NaCl (pH 6.8) as described.[10] Kinetic parameters were determined by varying the concentration of DD-ACP (0−24 μM) at a fixed concentration of NADH (250 μM) and by varying the concentration of NADH (0−250 μM) at a fixed, saturating concentration of DD-ACP (24 μM). Kinetic parameters were determined by fitting the initial velocity data to eq 1 using GraFit 4 (Erithacus Software Ltd.). Equation 1 allows *V*/*K* to be evaluated as a single parameter (VK), thus enabling the standard error for *V*/*K* to be directly determined.[28]

$$v_i = (V[S]VK)/(V + [S]VK) \quad (1)$$

Kinetic Isotope Effects. Primary kinetic isotope effects on *V* (^{D}V) and *V*/*K* ($^{D}(V/K)$) were determined at 25 °C in 30 mM PIPES and 150 mM NaCl (pH 6.8) at a fixed, saturating concentration of NADH or 4(*S*)-NADD (250 μM) and by varying the concentration of DD-ACP (0−24 μM). Alternatively, the kinetic isotope effects were determined at a fixed, saturating concentration of DD-ACP (24 μM) and by varying the concentration of NADH or 4(*S*)-NADD (0−250 μM). Kinetic isotope effects were calculated by fitting the initial velocity data to eq 2 using Grafit 4.[10]

$$v_i = V[A]/(K_A(1 + fi(E_{V/K})) + [A](1 + fi(E_V))) \quad (2)$$

In eq 2, *V* is V_{max}, [A] is the concentration of the varied substrate, fi is the fraction of deuterium in NADD, and $E_{V/K}$ and E_V are the isotope effects minus 1 on *V*/*K* and *V*, respectively. A value of 0.95 was used for fi.

Fluorescence Titration Experiments. Equilibrium fluorescence titrations were performed with a model FL3-21 Fluorolog-3 spectrofluorimeter (Edison, NJ). All measurements were carried out at 25 °C in 100 mM PIPES (pH 6.8). The excitation wavelength was 360 nm (5 nm slit width), and the emission wavelength was 440 nm (1 nm slit width). Briefly, 1 μL aliquots of 3 mM NADH were added to a 3 mL of solution of 1 μM protein. The fluorescence intensity was recorded as an average of 60 readings (2 s). For wild-type InhA data were fit to a quadratic equation as described previously.[7,10] For the F149A enzyme NADH binding curves were not hyperbolic, but sigmoidal. These data were analyzed by the Hill equation.[7,10]

Raman Spectroscopy. Raman spectra were acquired as described previously using 700 mW of 752 nm laser excitation.[19] Initially, 70 μL of enzyme (ca. 500 μM) was added to a quartz cell and 480 × 1 s scans were accumulated. Subsequently, 1 equiv of the NADD cofactor was added to form a binary complex, and the Raman spectrum measured. Then, 1 equiv of dienoyl-CoA (typically between 1 and 2 μL of about 20 mM concentration) was introduced into the same cell, and again the Raman spectrum was recorded. The Raman difference spectra of the bound cofactor were obtained by subtracting the spectrum of the enzyme from the spectrum of the binary complex. Similarly, the spectrum of the substrate analog was produced by subtracting the spectrum of the binary complex from that of the ternary complex. An appropriate scaling factor was applied to each subtraction to eliminate any residual protein signals. The difference spectra were wavenumber calibrated against cyclohexanone and deuterated chloroform and are accurate to ±2 cm^{-1}. The resolution of the Raman instrument is 8 cm^{-1}. The software used to acquire Raman spectra was WinSpec (Princeton Instrument), and spectral manipulations were performed using Win-IR.

Scheme 2. Conformations of the Model Nicotinamide Compounds used for the Calculations

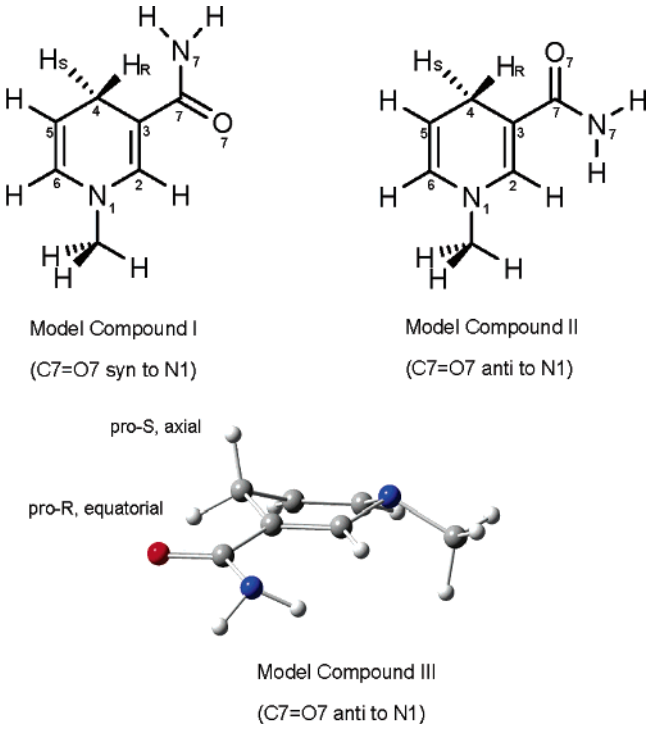

Density Functional Theory Calculations. Quantum chemical calculations were carried out using Gaussian 2003 with the Becke-3−Lee−Yang−Parr (B3LYP) DFT functional and the 6-31G** basis set.[29,30] This approach was used to both optimize the structure of the model compound *N*-methyl-1,4-dihydro-nicotinamide, (with deuterons at either the 4(*R*) or 4(*S*) positions) and calculate vibrational spectra. Calculations were performed for several conformations of the nicotinamide ring (Scheme 2). Both conformers I and II have planar nicotinamide rings with the carboxamide group either syn (I) or anti (II) to the ring nitrogen (N1). In conformer III, the C4 carbon is distorted 15° out of the plane of the ring and the carboxamide is in the anti conformation.

Results

Steady-State Kinetics Analysis of Wild-Type and F149A InhA Proteins. InhA and other enoyl reductases are routinely assayed using CoA-based substrates such as DD-CoA instead of substrates based on acyl carrier protein (ACP) due to the relative ease of synthesizing the enoyl-CoAs. However, recently we have discovered that enoyl-ACPs do not give rise to substrate inhibition in contrast to the corresponding CoA substrates. Consequently, DD-ACP was used in the present work in order to facilitate evaluation of ^{D}V. Steady-state kinetic parameters obtained using DD-ACP synthesized from *E. coli* ACP are given in Table 1, where it can be seen that F149A InhA mutant had a k_{cat} value that was reduced 30-fold compared to that of wild-type InhA. The F149A mutation had only a small affect on the K_m values for the two substrates, and the k_{cat}/K_{DDACP} and k_{cat}/

(28) Northrop, D. B. *Anal. Biochem.* **1983**, *132*, 457−461.

(29) Lee, C. T.; Yang, W. T.; Parr, R. G. *Phys. Rev. B* **1988**, *37*, 785−789.
(30) Becke, A. D. *Phys. Rev. A* **1988**, *38*, 3098−3100.

Table 1. Kinetic Parameters for Wild-Type and F149A InhA

enzyme	k_{cat} (min^{-1})	k_{cat}/K_{DDCOA} ($min^{-1}\ \mu M^{-1}$)	k_{cat}/K_{NADH} ($min^{-1}\ \mu M^{-1}$)	K_{DDCoA} (μM)	K_{NADH} (μM)	$K_{d\ NADH}$ (μM)
wild-type	190 ± 3	34.9 ± 3.2	5.4 ± 0.6	5.4 ± 0.6	35.2 ± 4.5	0.60 ± 0.09
F149A	6.55 ± 0.25	1.51 ± 0.25	0.43 ± 0.03	4.33 ± 0.88	15.2 ± 1.64	10.9 ± 1.7
ratio	29	23	13	1.2	2.3	0.055

Table 2. Vibrational Data for NADD Free in Solution and Bound to Wild-Type and F149A InhA

4(*S*)-NADD			4(*R*)-NADD	
C(4)–D stretch (cm^{-1})	fwhm (cm^{-1})		C(4)–D stretch (cm^{-1})	fwhm (cm^{-1})
2115	59	free, in solution	2111	52
2104	26	bound to wild-type InhA (binary complex)	2145	29
2106	23	bound to wild-type InhA (ternary complex[a])	ND[b]	ND[b]
2111	52	bound to F149A (binary complex)	2114	47

[a] Ternary complex with *trans*,*trans*-2,4-decadienoyl-CoA. [b] ND, not determined.

Table 3. Primary Kinetic Isotope Effects for Wild-Type and F149A InhA

enzyme	^{D}V	$^{D}(V/K_{NADH})$	$^{D}(V/K_{DDCoA})$
wild-type	1.87 ± 0.36	2.16 ± 0.82	2.23 ± 0.21
F149A	1.54 ± 0.25	4.74 ± 0.8	2.1 ± 0.87

K_{NADH} values were reduced 23- and 13-fold, respectively, compared to those of wild-type InhA.

Kinetic Isotope Effects. To further investigate the role of F149 in substrate reduction, we measured the primary kinetic isotope effects for wild-type and F149A InhA (Table 3). While the ^{D}V and $^{D}(V/K_{DDACP})$ values for wild-type and F149A InhA were the same, within experimental error, $^{D}(V/K_{NADH})$ was increased 2-fold for the F149A mutant.

Equilibrium Binding of NADH. Dissociation constants (K_d) for the interaction of NADH with wild-type InhA and F149A InhA were determined by fluorescence spectroscopy (Table 1).[7] For wild-type InhA, NADH binding curves were hyperbolic and K_d value obtained for wild-type InhA was 0.60 ± 0.09 μM, which is identical within experimental error to that reported earlier (0.57 ± 0.04 μM).[7] In contrast, NADH binding to the F149A InhA enzyme was not hyperbolic but sigmoidal, indicating that the cofactor binds cooperatively to the enzyme. Inspection of the binding curve indicated that NADH binding was 50% complete at 10.9 ± 1.7 μM NADH. Fits of the data to the Hill equation gave a Hill coefficient of 2.6 ± 0.2.[7]

Raman Spectroscopy. The Raman difference spectra of deuterium-labeled 4(*S*)-NADD in solution and bound to wild-type InhA are shown in Figure 2. Between 600 and 1700 cm^{-1} many vibrational bands can be observed which arise from different portions of the NADD molecule. The spectra closely resemble data previously presented and discussed by Callender and colleagues[14−17] and are only presented here to show the overall spectral quality and relative intensity of the C−D stretching vibration (ν_{C-D}), which can be observed at 2115 and 2104 cm^{-1} for free and bound 4(*S*)-NADD, respectively. Raman spectra were also obtained for 4(*S*)-NADD bound to F149A and for the corresponding enzyme complexes with the 4(*R*)-NADD isomer. The ν_{C-D} spectra are shown in Figure 3, whereas the band positions are band widths are summarized in Table 2. The frequency and bandwidth of the C−D bands for both 4(*S*)- and 4(*R*)-NADD are similar and are consistent with values previously reported by Callender and co-workers for the free

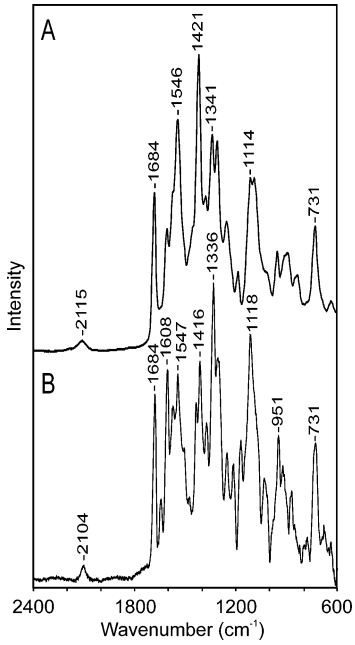

Figure 2. Raman difference spectra of 4(*S*)-NADD (A) in aqueous solution and (B) in a binary complex with wild-type InhA. The difference spectrum of NADD in solution was obtained by subtracting a Raman spectrum of the buffer.

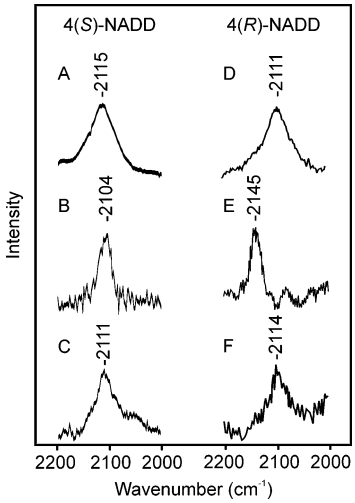

Figure 3. Raman difference spectra in the C−D stretching region of 2000−2200 cm^{-1}: (A) 4(*S*)-NADD in aqueous solution, (B) a binary complex of 4(*S*)-NADD and wild-type InhA, (C) a binary complex of 4(*S*)-NADD with F149A−InhA, (D) 4(*R*)-NADD in aqueous solution, (E) a binary complex of 4(*R*)-NADD and wild-type InhA, and (F) a binary complex of 4(*R*)-NADD with F149A−InhA. The difference spectra of NADD in solution were obtained by subtracting Raman spectra of the buffer.

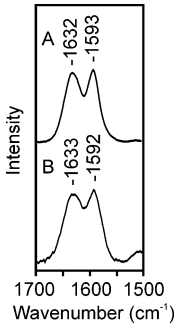

Figure 4. Raman spectra of *trans*,*trans*-2,4-decadienoyl-CoA in (A) aqueous solution and (B) bound to InhA in a ternary complex with NADH. A small contribution from NADH has been removed from the spectra. The difference spectrum of the ligand in solution was obtained by subtracting a Raman spectrum of the buffer.

cofactors.[14−17] However, whereas ν_{C-D} decreases 11 cm^{-1} when 4(*S*)-NADD binds to wild-type InhA, Figure 3 shows that ν_{C-D} actually increases 34 cm^{-1} for 4(*R*)-NADD upon binding (Table 2). Finally, formation of the ternary complex of 4(*S*)-NADD with InhA in the presence of the substrate analog, decadienoyl-CoA, results in no further change in ν_{C-D} (data not shown).

The effect of enzyme binding on NADD is also illustrated by the full width at half-maximum (fwhm) of the ν_{C-D} bands (Table 2), which yields information on the conformational flexibility of the cofactor. Overall, binding of 4(*S*)- and 4(*R*)-NADD to wild-type InhA causes the ν_{C-D} bands to narrow. The fwhm decreases from 59 cm^{-1} for 4(*S*)-NADD in solution to 26 cm^{-1} in the binary enzyme−NADD complex and 23 cm^{-1} in the ternary complex with decadienoyl-CoA. Similar changes in the fwhm are also observed for 4(*R*)-NADD, and the changes in fwhm indicate that the conformational flexibility of the cofactor is dramatically reduced on binding to the enzyme.

Replacement of the F149 residue in InhA with Ala results in a 30-fold reduction in k_{cat} and a 13-fold decrease in k_{cat}/K_{NADH}. To probe the mechanistic basis for these changes in kinetic constants, we measured the Raman spectrum of 4(*S*)- and 4(*R*)-NADD bound to F149A (Figure 3). In contrast to wild-type InhA, when 4(*S*)-NADD is bound to F149A, the C4(*S*)−D stretching band is observed at 2111 cm^{-1} with a fwhm of 52 cm^{-1}. Similar data were obtained for 4(*R*)-NADD, and thus, both the position and the fwhm of the C4−D stretching bands for the F149A−cofactor complexes are more similar to the values observed for NADD in solution than when bound to the wild-type enzyme (Table 2).

In a parallel set of Raman studies we examined the structure of a substrate analog, decadienoyl-CoA, in ternary complexes with NADH and InhA as shown in Figure 4. The Raman spectrum of decadienoyl-CoA in solution has two intense bands at 1593 and 1631 cm^{-1}. On the basis of extensive Raman studies with isotopically labeled hexadienoyl-CoA binding to enoyl-CoA hydratase and medium-chain acyl-CoA dehydrogenase (MCAD), we can assign the bands at 1593 and 1631 cm^{-1} to modes involving the in-phase and out-of-phase combinations of the two C═C stretching coordinates which are also coupled to the C═O stretching coordinate. For enoyl-CoA hydratase and MCAD, binding results in a ground-state polarization of hexadienoyl-CoA representing activation of the ligand.[20] Surprisingly, on binding to InhA, with or without NADH (Figure 4) or NAD^+ (data not shown), there is no significant shift in the position of the decadienoyl-CoA Raman bands. The lack of any significant change in the vibrational band positions of the substrate analog on binding to InhA indicates that either ground-state substrate distortion is not a significant contributor to catalysis, as suggested by Fillgrove and Anderson,[11] or that the substrate analog does not sufficiently well duplicate the structure of the true substrate to reveal enzyme−substrate interactions important for catalysis.

Table 4. Calculated Changes in Vibrational Stretching Frequencies between Compounds II and III[a]

	$\Delta\nu_{C-D}$ (cm^{-1})	
method	axial	equatorial
B3LYP[b]	−17	+26
MINDO/3[c]	−14	+18
AM1[c]	−5	+11

[a] $\Delta\nu_{C-D}$ is the change in C4−D stretching frequency on binding. [b] Using the 6-31G** basis set. [c] Taken from ref 14.

Table 5. Calculated Changes in Vibrational Stretching Frequencies between Compounds I and III[a]

	$\Delta\nu_{C-D}$ (cm^{-1})	
method	axial	equatorial
B3LYP[b]	+3	+45
MINDO/3[c]	+8	+40
AM1[c]	+4	+33

[a] $\Delta\nu_{C-D}$ is the change in C4−D stretching frequency on binding. [b] Using the 6-31G** basis set. [c] Taken from ref 14.

Density Functional Theory Calculations. In order to assess the impact of distorting the nicotinamide carbon out of the ring plane, we used DFT methods to calculate the vibrational stretching frequency (ν_{C-D}) of the pseudoaxial and pseudoequatorial C4−D bonds for the three model compounds shown in Scheme 2. These calculations predict that a 15° distortion of the C4 carbon out of the ring plane will result in a 17 cm^{-1} decrease and 26 cm^{-1} increase in ν_{C-D} for the pseudoaxial and pseudoequatorial bonds, respectively, when the carboxamide group is in the anti conformation (model compound II to III, Table 4). In addition, when the out of plane distortion of the C4 carbon is accompanied by rotation of the nicotinamide carboxamide group from a syn to an anti conformation, (model compound I to III), the calculations indicate that ν_{C-D} will increase for both the pseudoaxial and pseudoequatorial bonds by 3 and 45 cm^{-1}, respectively (Table 5). These DFT calculations are in good agreement with the semiempirical calculations originally performed by Deng et al.[14]

Discussion

NADD Binding to Wild-Type InhA. The Raman spectra of 4(*R*)- and 4(*S*)-NADD in solution show very broad ν_{C-D} bands that have similar vibrational frequencies (Table 2). On binding to InhA, there is a dramatic reduction in the fwhm of the ν_{C-D} bands (Table 2). The narrowing of these bands indicates that the nicotinamide ring, which exists as a population of rapidly interconverting conformers in solution in which the C4−D bonds are both pseudoaxial and pseudoequatorial, is conformationally constrained upon binding to InhA. In order to determine the conformation of the bound cofactor, we must consider the effect of ring puckering and orientation of the carboxamide group on ν_{C-D}.[14−17]

Raman spectra of 4(*R*)- and 4(*S*)-NADD show that upon binding to wild-type InhA, ν_{C-D} for the C4(*S*)−D bond

decreases 11 cm^{-1}, whereas ν_{C-D} for the C4(*R*)−D bond increases 34 cm^{-1} (Table 2). On the basis of the DFT calculations (Table 4), these data are thus consistent with the C4(*S*)−D and C4(*R*)−D bonds adopting pseudoaxial and pseudoequatorial orientations, respectively, on binding to InhA. The correlation with the experimental data is particularly good when the DFT calculations on compounds II and III are used, in which the carboxamide group is maintained in the anti conformation (model compound II to III).

However, while the carboxamide group is anti to the nicotinamide ring in crystal structures of NADH bound to InhA,[5] Fischer et al. have proposed that the carboxamide group is syn in solution.[31] If this is so, then the binding of NADH to InhA must be accompanied by a syn to anti rotation of the nicotinamide carboxamide group. While the calculations still predict a significant binding-induced increase in ν_{C-D} for the C4(*R*)−D bond (compounds I and II, +45 cm^{-1}), inclusion of syn to anti rotation of the carboxamide predicts a small 3 cm^{-1} increase in ν_{C-D} for the C4(*S*)−D bond rather than the observed 11 cm^{-1} decrease (Table 5). The discrepancy between theory and experiment is not large, and we note that in the X-ray structure the amide is bent out of the ring plane by 20° (Figure 1), which could have an additional impact on ν_{C-D} that is not accounted for in the calculations.

InhA is a B-type reductase and transfers the pro-4(*S*) hydrogen to the substrate. Our conclusion that InhA binds NADD in a conformation in which the C4(*S*)−D bond is pseudoaxial to the ring is consistent with separate studies by Nambiar et al. and Almarsson and Bruice in which it was proposed that hydride transfer is assisted by placing the appropriate C4−H bond in a pseudoaxial orientation.[32,33] Thus, one method InhA employs to promote catalysis is to the productively bind the cofactor in a conformation which is optimized for hydride transfer. The similarity in both ν_{C-D} and fwhm for the ternary complex obtained using *trans*,*trans*-2,4-decadienoyl-CoA (Table 2) implies that the enzyme−substrate complex is already fully organized when only the NADH cofactor is bound.

The ability of enzymes to bind NADH in the correct geometry for hydride transfer has been previously observed in other dehydrogenases using Raman spectroscopy.[16,17] In addition, Beis et al. have reported the 1.5 Å structure of NADH bound to dTDP-D-glucose dehydratase, another member of the SDR superfamily (PDB code: 1OC2).[34] In this structure, the nicotinamide ring adopts a boat conformation which orients the C4 carbon and N1 nitrogen atoms 20° and 30° out of the ring plane, respectively. This places the catalytically active C4−H bond in a pseudoaxial conformation optimized for hydride transfer to the substrate.

NADD Binding to F149A−InhA. InhA is a member of the SDR family.[1−3] All members of this family have a conserved catalytic triad consisting of a tyrosine and lysine residues. In the dehydrogenases the third residue is a Ser or Thr, while in the enoyl reductases this residue is either a Phe, as in InhA, or a Tyr, as in FabI, the enoyl reductase from *E. coli*. In the crystal structure of the wild-type InhA−NADH complex, the cofactor binds at the bottom of a large open cavity and the benzyl side chain of residue F149 lies just above the nicotinamide ring[5] (Figure 1). The proximity of F149 to the NADH nicotinamide ring suggests that this residue may be involved in controlling the conformation of the bound cofactor. In support of this hypothesis, ν_{C-D} for 4(*R*)- and 4(*S*)-NADD bound to F149A−InhA closely resemble the corresponding bands for NADD in solution. Thus, whereas binding to wild-type InhA causes a 50% reduction in the fwhm values of both C4−D bands, NADD bound to F149A−Inha shows a reduction of fwhm of only 10% (Figure 3). Additionally, the significant changes in ν_{C-D} seen with the binding of NADD to wild-type InhA are virtually absent in the F149A enzyme complexes. In particular, whereas wild-type InhA causes the ν_{C-D} of 4(*R*)-NADD to increase by 34 cm^{-1}, F149A−InhA causes only a 3 cm^{-1} increase in frequency. Thus, we conclude that F149 is directly involved in controlling the conformation of the nicotinamide ring.

In order to shed more light on the role of F149 in catalysis, we have determined the primary isotope effects on ^{D}V and $^{D}(V/K)$ using NADD as a substrate. Previous experiments have relied on the use of CoA-based substrates, but here we replaced DD-CoA with DD-ACP since the latter substrate does not give rise to substrate inhibition. For the wild-type enzyme, ^{D}V, $^{D}(V/K_{NADH})$, and $^{D}(V/K_{DDACP})$ have similar values, within experimental error, consistent with a mechanism in which NADH and DD-ACP bind randomly to the enzyme. In addition, the small normal values observed for the latter isotopes effects are consistent with a stepwise mechanism in which both hydride transfer and protonation of the enolate intermediate are partially rate limiting. Interestingly, when F149 is replaced with an Ala the only significant change in the measured primary isotope effects is on $^{D}(V/K_{NADH})$, which increases from 2.1 in wild-type InhA to a value of 4.9 for the mutant (Table 3). The effect on $^{D}(V/K_{NADH})$ can be accounted for by proposing the mutation has both decreased the external commitment factor for NADH and destabilized the transition state for hydride transfer, resulting in an increase in the primary kinetic isotope effect for this step. Since the Raman data indicate that the F149A mutant is unable to productively orient the nicotinamide ring in the active site, the increase in $^{D}(V/K_{NADH})$ thus supports a direct link between the conformation of the NADH ring and the hydride transfer reaction.

While the above argument is attractive, we must also account for the observation that ^{D}V and $^{D}(V/K_{DDACP})$ are not affected by the mutation. The fact that $^{D}(V/K_{NADH})$ is affected while $^{D}(V/K_{DDACP})$ remains unchanged is consistent with the cofactor binding experiments which show the affinity of NADH for the enzyme is significantly reduced in the F149A mutant. For the wild-type enzyme, NADH and ACP substrate dissociate with similar rates from the ternary complex, suggesting both the cofactor and substrate have similar external commitments. Alternatively, for the mutant, NADH dissociates more rapidly than the ACP substrate, thereby decreasing the external commitment of the cofactor to catalysis. This explanation suggests that binding of cofactor to the wild-type enzyme is partially rate limiting, a result which is consistent with evidence that NADH binding causes a conformational change of the protein (unpublished data). Finally, the lack of effect on ^{D}V suggests the F149A mutation has not only raised the barrier to hydride transfer but also must have decreased the rate constant for a

(31) Fischer, P.; Fleckenstein, J.; Hones, J. *Photochem. Photobiol.* **1988**, *47*, 193−199.
(32) Nambiar, K. P.; Stauffer, D. M.; Kolodziej, P. A.; Benner, S. A. *J. Am. Chem. Soc.* **1983**, *105*, 5886−5890.
(33) Almarsson, O.; Bruice, T. C. *J. Am. Chem. Soc.* **1993**, *115*, 2125−2138.
(34) Beis, K.; Allard, S. T. M.; Hegeman, A. D.; Murshudov, G.; Philp, D.; Naismith, J. H. *J. Am. Chem. Soc.* **2003**, *125*, 11872−11878.

step following the first irreversible step, for example, product dissociation or protonation of the enolate intermediate, if hydride transfer is effectively irreversible.[11,35]

Ternary Complexes of InhA with NADH and a Substrate Analog. In the second series of experiments we have probed the effect of InhA on the ground-state structure of a substrate analog, decadienoyl-CoA. Surprisingly, there is no evidence for any ground-state activation in this system despite the fact that the carbonyl oxygen of the substrate oxygen is believed to be directly involved in two hydrogen bonds with Y158 and the 2′-hydroxyl of the ribose ring of NADH.[2] By comparison, two enzymes from the β-oxidation pathway with similar hydrogen bonding arrangements, enoyl-CoA hydratase and MCAD, were both found to strongly activate the ground-state structure of a diene analog, hexadienoyl-CoA.[18−21] However, Fillgrove and Anderson have proposed that enoyl and dienoyl reductases, where the proton-transfer step is rate limiting, may not require stabilization of enol(ate) or dienol(ate) intermediates, as this would be unfavorable for the proton-transfer step.[11]

Conclusion

In summary, Raman spectroscopy has demonstrated that the bound NADH cofactor, in binary and ternary complexes with wild-type InhA, is conformationally restricted such that the C4-(*S*) bond of the nicotinamide ring adopts a pseudoaxial orientation. Replacement of F149 with Ala correlates with a 30-fold decrease in k_{cat} which KIE data suggest results from an increased energy barrier to hydride transfer and decrease in the external commitment factor for NADH. In addition, KIE data indicate that the F149A mutation is also associated with the increase in energy barrier for a step following hydride transfer, such as protonation of the enolate intermediate or product dissociation. Site-directed mutagenesis coupled with primary kinetic isotope effect data thus indicates that F149, a member of the InhA catalytic triad, plays a critical role in lowering the energy of the transition state by correctly orienting the NADH cofactor to its most active form for hydride transfer.

Acknowledgment. This work was supported by Grants from the National Institutes of Health (GM63121 and AI44639, P.J.T.). P.J.T. is an Alfred P. Sloan Research Fellow. C.F.S. is a Howard Hughes Medical Institute Research Fellow. In addition, this material is based upon work supported in part by the U.S. Army Research Office under Grant DAAG55-97-1-0083. We are grateful to Deborah Stoner-Ma for her assistance with some of the Raman experiments. We also thank the reviewers for their insightful comments.

JA068219M

(35) Cook, P. F.; Cleland, W. W. *Biochemistry* **1981**, *20*, 1790−1796.
(36) Delano, W. L. http://www.pymol.org, 2002.